PCCP

PAPER

Cite this: *Phys. Chem. Chem. Phys.*, 2017, **19**, 8243

On the coupling between the dynamics of protein and water†

Yulian Gavrilov, Jessica D. Leuchter and Yaakov Levy*

Interactions between water and biomolecules can significantly change the former's structural, dynamic, and thermodynamic properties relative to the bulk. Experimental, theoretical, and computational studies show that changes in water properties can be observed at distances of more than 10 Å from a biomolecule. The effects of biopolymers on hydration water molecules can be attributed to several factors: the chemical nature of the amino acid residues involved, the spatial arrangement of the biomolecule, and its conformational flexibility. In the current study, we concentrate on the effect of protein chain flexibility on the properties of hydration water, using short peptides as a model. We constructed 18 linear peptides with the sequence (XXGG) × 5, where X represents one of the common amino acids, other than glycine and proline. Using molecular dynamics (MD) simulations, we studied how restricting the chain flexibility can affect the structural, dynamic, and thermodynamic properties of hydration water. We found that restricting the peptide dynamics can slow down the translational motions of water molecules to a distance of at least 12–13 Å. Analysis of the 'slow' water molecules (residence time ≥ 100 ps) together with a thermodynamic analysis of water within 4.5 Å of the peptide revealed significant differences between the hydration properties of the peptides. The balance between the entropic and enthalpic solvation effects defines the final contribution to the hydration free energy of the restricted system. Our study implies that different regions of the proteins that have different configurational entropies may also have different solvation entropies and therefore different contributions to the overall thermodynamic stability. Therefore, mutations of a solvent exposed residue may modify the thermodynamic stability depending solely on the flexibility of the mutated sites due to their different solvation characteristics.

Received 9th November 2016,
Accepted 1st March 2017

DOI: 10.1039/c6cp07669f

rsc.li/pccp

Introduction

Water plays an important role in the functioning and stability of proteins and other biological molecules.[1–4] Most proteins and nucleic acids are functional only in aqueous solution, and their stability and conformational flexibility are also strongly affected by water. For example, water–protein interactions govern processes such as protein folding, mediation of protein's interactions with other molecules, and acceleration of enzymatic activity.[1,3–11] Therefore, the activity of a protein is significantly modulated by the structure and dynamics of the surrounding water. Water may strongly modulate the protein dynamics. The link between the dynamics of a protein molecule and its hydration water has been studied using computational and experimental approaches[12–20] and was found to be tight. However, the origin of this coupled dynamics is not entirely clear. It was shown that the protein dynamics is '[en]slaved' to the motion of the bulk water.[15,21] On the other hand, other studies, suggested that the protein and hydration water have a mutual effect on each other's motions.[12,22–26]

Coupled motions of a protein and its hydration shell occur on several time scales. Time resolved fluorescence (femtosecond) spectroscopy identified two types of water-network relaxations in the protein hydration shell.[14,27–30] The first, occurring on a timescale of a few ps, results from local collective H-bond network relaxation. Hindered femtosecond motions of water in the bulk are highly suppressed and slow down close to the protein surface. The second type of relaxation, occurring on a timescale of tens to hundreds of ps, results from lateral cooperative rearrangements and is related to the coupled interfacial water–protein motions. It has been suggested that multiple relaxation rates and residence time distributions in the protein hydration shell exist because of the structural and chemical heterogeneity of the protein surface.[31,32]

Department of Structural Biology, Weizmann Institute of Science, Rehovot 76100, Israel. E-mail: Koby.Levy@weizmann.ac.il; Tel: +972-8-9344587

† Electronic supplementary information (ESI) available: Tables with average water residence time constants, amplitude-weighted average residence times and amplitudes of hydration water molecules. Figures: distribution of the number of water molecules within a certain cutoff distance from the RRGG peptide surface; the average time it takes a water molecule to reach a certain distance from the peptide surface; and thermodynamically favorable hydration sites on the surface of different peptides. See DOI: 10.1039/c6cp07669f

Biphasic protein hydration dynamics is consistent with neutron scattering data,[12,33,34] NMR studies[35] and MD simulations[36] (see also ref. 37–46). However, other studies suggest that the long decay component of hydration dynamics is caused solely by protein motions or by the trapped water molecules.[47–50]

Another interesting observation to emerge from femtosecond spectroscopy studies is that the dynamic hydration layer extends to more than 10 Å,[14] which is in agreement with THz spectroscopy studies[51] that showed that the diameter of such a hydration shell can exceed 10–20 Å for a folded protein.[52,53] MD simulations relate the experimentally observed changes in THz absorption in the solvation shell of proteins to the strengthened interactions among water molecules. Nevertheless, the changes in water dynamics were observed only up to a distance of 7–8 Å from the protein surface.[53] Generally MD simulations reveal no difference between the hydration water and the bulk beyond 10 Å.[53–58] However, some computational studies demonstrate the difference in water for longer distances. The retardation of the dielectric response of hydration water around an Ala peptide extends for more than 10 Å.[18] Spatial correlation between the protein and collective water dipoles can extend out to 40–50 Å[59] and the size of the hydration shell may correlate with the protein dipole moment.[60]

The chemical composition of the protein surface, its secondary structure, and spatial conformation are reflected in the structural and dynamical characteristics of its hydration shell.[61–64] MD simulations obtained by modulating protein dynamics and protein–water electrostatic interactions showed that water dynamics can be affected both by protein topological and energetic inhomogeneity.[65]

Different proteins may have very similar hydration dynamics. This arises from the similar local surface topology and surface chemical composition of many globular proteins,[66–70] whose surface composition is dominated by hydrophobic sites and H-bond donors, which results in a moderate slowdown of the fastest 90% of the water molecules. The dynamics of the remaining 10%, which consist of slow-moving water molecules is related to H-bond acceptor sites and deeply buried sites (for internal water).[66] Although only the first hydration layer was analyzed, the perturbations induced by the biomolecule do not fall away after 1–2 hydration layers and affect the collective motions of hydration water. The chemical nature of certain amino acid residues is a fundamental factor that defines their effect on hydration water; at the same time one should take into account the local environment of the residues. The mixture of effects related to the presence of polar groups and the amphiphilic character of molecules defines the complex effect of proteins on water.[71–73]

For example, for the three-helical villin headpiece subdomain it was shown that relaxation of the solvation time correlation function is significantly different for identical polar residues at different positions with different solvent exposure.[63] The same effect was observed for lysozyme[74] and myoglobin[14] proteins. The importance of the local environment for the hydration water dynamics is vividly demonstrated by the experimental and computational studies of antifreeze proteins (AFPs).[55,75–84] Ice recognition is usually performed on the ice binding surface which tends to be flat and relatively hydrophobic.[75] The preconfigured solvation shell around the ice binding proteins is involved in the initial recognition and binding of the AFP to ice by lowering the binding barrier and consolidation of the protein–ice interaction surface.[55]

Another indication of importance of the local environment is the difference in hydration of the native and non-native conformations of a protein. It was shown in experimental[14,85] and simulation[64] studies that solvation dynamics of the molten globule state can be faster or slower than the native state depending on whether the probe region becomes exposed or buried during the unfolding process. A general increase of the hydrated interface and less restriction of water dynamics were detected for the unfolded barstar protein.[86,87] THz spectroscopy study indicates that the dynamic hydration shell becomes less pronounced or even disappears for non-native conformations.[52,53] Alteration of hydration shell dynamics in a non-native conformation is also supported by studies of mutated proteins.[88,89]

Studying the dynamics of hydration water around intrinsically disordered proteins (IDPs) may improve the understanding of the connection between the spatial conformation, chemical composition of a protein and hydration water dynamics. The large content of hydrophilic residues prevents the hydrophobic collapse of IDPs and results in a solvent accessible area that exceeds that of folded globular proteins by several times.[90] The extended conformation of IDPs and intensive interaction with water may result in different hydration effects in comparison to the folded proteins.[12] Thus, computational studies suggest that IDPs may lower the hydration free energy. Stronger motional flexibility of IDPs compared with folded proteins is combined with more restricted water motions on the protein surface.[22] More accurately, the high conformational flexibility of IDPs facilitates higher mobility of the surrounding water molecules, while exposure and abundance of the charged residues confines them within the hydration layer.[56,91] It is possible to say that dynamics of water and IDPs is highly coupled. Studies of IDPs demonstrate that along with the topological and energetic inhomogeneity the flexibility of the protein can sufficiently affect the characteristics of the hydration water and result in important biological effects.

If the protein flexibility is absent, the degree of restriction of the hydration water dynamics of both IDPs and globular proteins increases.[92] Direct manipulations with the protein conformational flexibility and protein–water interactions using a computational approach help to understand the coupling between protein and hydration water dynamics. MD simulations were used to study how the conformational flexibility and protein–water electrostatic interactions at the surface of the protein influence the hydration water.[65,93–96] It was shown that hydration water dynamics around a protein can be slowed down by restriction of protein dynamics. If protein–water electrostatic interactions are eliminated, water reorientational dynamics can become even faster than in the bulk.[65]

The studies summarized above suggest that hydration properties are strongly connected to the properties of the solute

(*i.e.*, the protein), including its chemical composition (the identity of its amino acid residues), its spatial organization (secondary and tertiary structures), and its conformational dynamics. Because these properties are interconnected, it would be valuable to study a model system that will enable the roles of these factors to be separately quantified. This study aims to dissect the pure contribution of protein flexibility on hydration dynamics. When comparing water dynamics around IDPs and globular proteins, it is difficult to dissect the contributions of flexibility, protein shape, and amino acid composition to water dynamics. For example, the shape of globular proteins may have steric effects that affect water dynamics. Similarly, the higher content of polar or charged amino acids in IDPs may have an effect on the solvent.

In the present study, we concentrated on the effect of protein dynamics on its hydration by comparing the characteristics of the hydration shell around short and linear peptides that have the same structure but different flexibility. We studied the effect of chain composition and flexibility on the hydration shell of peptides of 20 amino acid length that share the sequence XXGG (repeated 5 times), where X represents any common amino acid except glycine or proline. Using atomistic MD simulations, we studied the solvation of flexible and restrained versions of each constructed peptide (Fig. 1). This model allowed us to study the coupling between protein and water dynamics for different peptide sequences while eliminating any effect of peptide conformation. Such a model would be valuable to obtain a systemized understanding of the effect of amino acid conformational flexibility within the polypeptide chain on hydration water by isolating the tight linkage between protein sequence and structure. Understanding how the free energy of residue–water interactions depends on the local flexibility of a mutated site is important for protein design and in particular for optimizing loop sequences.

Methods

The studied peptides were generated using Pymol version 1.7.0.5.[97] Each peptide is 20 amino acids long and repeats an identical XXGG sequence five times, where X represents a common amino acid other than glycine or proline (*i.e.*, X is any one of the 18 different amino acids). Two versions of each peptide were studied: one was flexible (we constrained only the dynamics of the N and C terminals) and the other was constrained. We restrained the dynamics of all the heavy atoms with the force constant of 1000 kJ mol^{-1} nm^{-2}. Such a restriction does not totally confine the peptide motions but allows some fluctuations of the atoms' positions. We thus produced 36 different systems (18 flexible and 18 constrained). The conformation of the constrained version of each of the peptides was chosen based on the distribution of the internal energy for different conformations that were obtained during the MD simulation involving the flexible versions of the peptides at 300 K. In each case, a conformation with the most populated internal energy value was chosen to perform the constrained simulation. In order to check the effect of a specific conformation, for one system $(WWGG)_5$ (hereafter, WWGG, as well as for other peptides), we used two different constrained conformations. The analyses did not show any significant difference.

All-atom MD simulations were performed using the GROMACS package version 5.0.4 with the AMBER99SB-ILDN force field.[98,99] The linear constraint solver (LINCS) algorithm was used to control bond lengths during the simulation.[100] Sodium or chloride ions were added to achieve charge neutrality. To integrate the equations of motion, the leapfrog algorithm was used with steps of 2 fs. A modified Berendsen thermostat[101] was used to control the temperature at 300 K. Explicit water molecules were added. We used the extended simple point charge (SPC/E) model

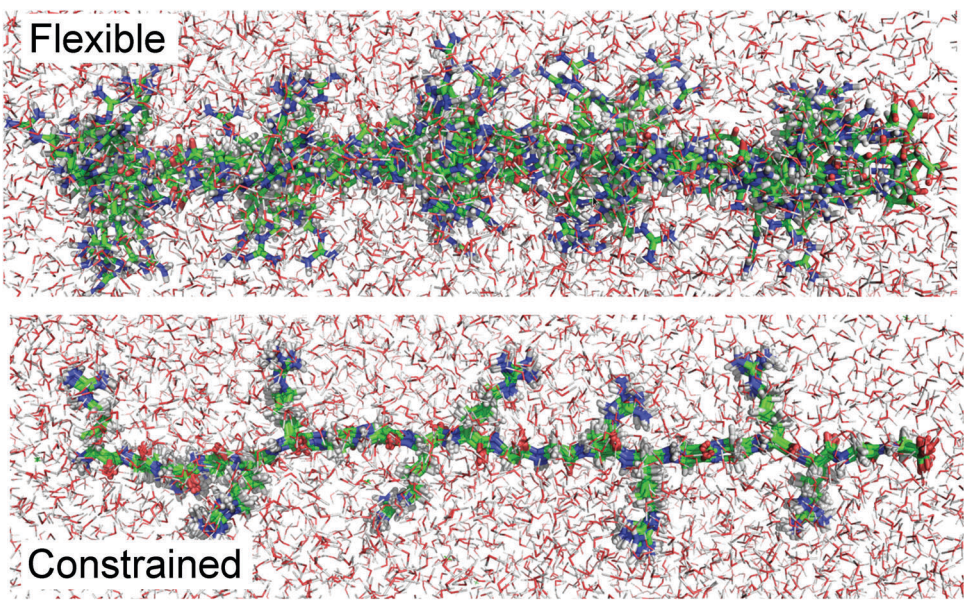

Fig. 1 Graphical representation of the constructed peptides using RRGG as an example. Flexible (top) and constrained (bottom) versions of RRGG are shown as ten aligned conformations represented as sticks and surrounded by water molecules represented as lines.

for all systems because analysis has shown that the SPC/E water model gives the best bulk water dynamics and structure when compared with the experimental values of liquid water.[102] Also, the SPC/E water model shows the relaxation of water more accurately.[103] In addition, we checked for the effect of the water model by repeating the simulations for the RRGG peptide using the five-site potential functions (TIP5P) water model.

Periodic boundary conditions were implemented by using the triclinic box and solvating the peptide in the presence of sodium or chloride ions with water so that the distance of any peptide atom is at least 15 Å from the edges of the box. In both the constrained and flexible peptides, the C_α atom at both the N and C terminals was fixed in space. Thus, both the constrained and flexible versions of the peptides were localized in space. The difference between the versions lay in the dynamics of the remaining heavy atoms. The structures were relaxed using the steepest descent method of energy minimization. Then, the systems were equilibrated in two steps (100 ps per phase). The first step was conducted in an *NVT* ensemble and the second phase in an *NPT* ensemble. In the next step, we performed long MD simulations in an *NPT* ensemble. For each system (*i.e.*, for 18 flexible and 18 constrained variants), we preformed 1 simulation for 100 ns.

Throughout this article, we use the peptide RRGG (Fig. 1) as an example when visually presenting the dynamic properties of the studied peptides. Flexible and constrained versions of the peptide are represented by overlapping ten different conformations throughout the simulation. One can see that the difference in the flexibility of the versions is primarily due to the dynamics of the side chains. The constrained peptide still has some slight flexibility in the side chains, which were less affected by spatial fixation of the heavy atoms.

We used the obtained 100 ns trajectories to calculate the tetrahedral order parameter, the radial distribution function of water molecules, the number of water molecules within the hydration shell, the survival probability of water molecules, the hydrogen bond autocorrelation function, and the thermodynamic parameters of hydration water.

Tetrahedral order parameter

The tetrahedral order parameter was used to determine the tetrahedral arrangement of the four closest neighbors to a given water molecule[104]

$$q_{\text{tet}} = 1 - \frac{3}{32}\sum_{j=1}^{3}\sum_{k=j+1}^{4}\left(\cos\varphi_{j,k} + \frac{1}{3}\right)^2$$

where $\varphi_{j,k}$ represents the angles formed around the oxygen atom of a given water molecule by the four hydrogen atoms closest to it: two hydrogens from its own molecule and two hydrogens from the two closest water molecules (j, k). The values $q_{\text{tet}} = 1$ corresponds to the perfect tetrahedral and $q_{\text{tet}} = 0$ corresponds to a random arrangement.

Radial distribution function

The radial distribution function (RDF; g(AB)) was used to determine the density and organization of water around the protein as a function of distance. It can be presented in terms of the relative number density (ρ) of water $g(\text{AB}) = \dfrac{\langle\rho\text{B}(r)\rangle}{\langle\rho\text{B}\rangle\text{local}}$. The numerator represents the particle density of B around particle A at distance r, and the denominator represents the averaged particle density of B over all spheres within a radius of $r_{\max}$ from particle A.

We used two versions of this function: (1) A represents heavy atoms of the peptide and B represents all water oxygens in the system; (2) A and B both represent the oxygen atoms of water molecules within the hydration shell of the protein. The cutoff distance for the hydration shell was chosen to be 5 Å from the protein surface.

The actual equation that was used to calculate the RDF is:

$$g(r) = \frac{2}{N(N-1)}\frac{1}{V_{\text{shell}}F}\sum_{i=1}^{N}\sum_{j=1}^{i-1}G(k_{ij})$$

where r is the distance between particles of type A and B; N is the total number of particles; and k_{ij} is the distance between particles i and j. In case (1), r refers to the distances between the protein and water molecules and k refers to the distances in between water molecules; in case (2), $r \equiv k$ and both A and B represent water molecules. F is a normalizing factor related to the usage of many microstates (snapshots of a trajectory) and to the density distribution of water molecules without a solute, assuming a homogenous density (specific to the applied water model).

The volume of the spherical shells (V_{shell}) located at different distances r from the particles of type A is given by

$$V_{\text{shell}}(r) = \frac{4}{3}\pi\left((r+\Delta r)^3 - r^3\right)$$

where Δr represents the difference in radius for consecutive spherical shells.

The function that defines whether particles i and j are within the distance between r and $r + \Delta r$ is given by

$$G(k_{ij}) = \begin{cases} 1, & \text{if } k_{ij} \le \Delta r \\ 0, & \text{if } k_{ij} > \Delta r \end{cases}$$

Survival probability

Survival probability (S) was used to determine the residence time of water molecules within a specified region. This function characterizes the relaxation dynamics of water molecules around the peptide or in the bulk. It may be expressed as

$$S(t) = \frac{\sum_{i=1}^{N} P(i, t_0, t_0 + t_1, t_0 + t_2 \ldots + t_0 + t_n)}{\sum_{i=1}^{N} P(i, t_0)}$$

where P in the numerator equals 1 if the water molecule (i) at time (t) was continuously present within the hydration shell starting from time t_0, otherwise $P = 0$; P in the denominator represents the water molecules (i) present at time t_0 in the hydration shell and equals 1. N is equal to the number of water

molecules within the hydration shell at time t_0; and n is equal to the total number of frames. Accordingly, $S(t)$ decreases in time from 1 to 0 if all water molecules initially present within the hydration shell leave it after some time.

For the peptides, water molecules were selected based on the distance between the water oxygen atoms and the peptide heavy atoms, for different cutoff distances, *i.e.* 3.5 Å, 5 Å *etc.* For bulk, water molecules were selected in a layer beyond a sphere with a radius of 50 Å (approximate radius of the peptide). Thus, we calculated the residence time of water molecules within the spherical shell whose width was equal to the cutoff distance. The center of the sphere is a reference water molecule. This way the number of analyzed water molecules close to the peptide and in the bulk was comparable.

Hydrogen bond autocorrelation function

The hydrogen bond autocorrelation function (C_{HB}) was calculated to track the dynamics of hydrogen bonds within the hydration shell of the peptides. It was calculated in the same way as the survival probability with an additional two cutoffs that determine the hydrogen bond and can be represented by

$$C_{\mathrm{HB}}(t) = \frac{\sum_{i=1}^{N} P(i, t_0, t_0 + t_1, t_0 + t_2 \ldots + t_0 + t_n)}{\sum_{i=1}^{N} P(i, t_0)}$$

Hydrogen bonding was considered to have occurred between two water molecules if the inter-oxygen distance was less than 3.5 Å and the smallest of the four HO$\cdots$O angles was less than 30°.

To improve the input data, autocorrelation functions (survival probability and H-bonds) were calculated for each nanosecond of the 100 ns runs and then averaged. The survival probability and H-bond autocorrelation functions relaxed long before reaching 1 ns, so we do not expect any loss of information.

Calculation of thermodynamic parameters

The thermodynamic parameters of hydration water were obtained using the grid inhomogeneous solvation theory (GIST) toolbox[105] from AMBER, a molecular dynamics package. The entropy of the peptide chain was estimated from the distributions of the backbone and sidechain dihedral angles (ϕ,ψ,χ). The entropy is then

$$S_{\mathrm{conf}} = -kT \sum_{j} \sum_{i}^{N} p^j(\alpha_i) \ln p^j(\alpha_i)$$

where the sum is over the N bins of the dihedral angle α_i of residue j and p is the population of the ith bin. The angles were discretized in bin sizes of 18°, 24°, and 36°. Very small differences in entropy were obtained for different bin sizes. The results are presented for a bin size of 24°. This method for estimating protein conformational entropy (or similar variants of it) has been successfully applied in different studies.[106–111] Two studies[107,109] found that motions in proteins are nearly uncorrelated, so we did not use joint probability distributions and assumed that the only contribution to the entropy was from the independent motion of the angle.

Results

Structural properties of hydration water

To estimate the effect of the restrained conformational dynamics of the peptides on the structural characteristics of the first layers of hydration water, we calculated the RDF of the water molecules and the tetrahedral order parameter. These structural properties, although limited in their sensitivity, should be examined before one moves to quantify the dynamic properties of the hydration water. The RDF analysis did not reveal any density distribution differences between the flexible and constrained versions of the peptides. See, for example, Fig. S1 (ESI†), which shows the RDF of hydration water around the peptide RRGG (only the water molecules within 3.5 Å from the peptide are included, convergence to one is not expected). The RDFs of all simulated water molecules around the flexible and constrained peptide atoms were indistinguishable. The average tetrahedral order parameter of water molecules as a function of water–protein distance showed no reliable difference in the distributions for flexible *versus* constrained versions of the peptides. See Fig. S2 (ESI†) for the RRGG example. Some difference in the fluctuation of this parameter immediately adjacent to the protein surface may be related to protein atoms not being considered in the calculation of tetrahedrality. Stronger retardation of water molecules close to the restrained peptides, especially in the first hydration shell (see the next section), may slightly affect this parameter.

In the modeled systems, the spatial fixation of the N and C terminals means that the main source of conformational flexibility is the dynamics of the side chains of the peptides. The absence of any pronounced difference in the RDF and tetrahedral order parameter after restriction of peptide flexibility indicates that sidechain flexibility is insufficient to affect the structural characteristics of the hydration water. No significant effect was observed for all residue types (all 18 modeled peptide types).

In addition, we investigated how restriction of the conformational dynamics can affect the number of hydration water molecules present within different distances around the peptides. The analysis showed that, for some peptide types, the difference in these numbers for flexible and constrained versions can change as a function of distance. This was shown for WWGG, EEGG, SSGG, QQGG, AAGG, LLGG, MMGG, FFGG, and YYGG. See Fig. S3 (ESI†) for the distributions of the number of water molecules at different distances from the RRGG peptide. However, it was revealed that this difference usually did not exceed 2% of the average values. Such a small difference is in agreement with the results of other structural analyses (RDF and tetrahedral order parameter). For some peptides, even such a difference was not observed (HHGG, VVGG, IIGG, KKGG, DDGG, TTGG, CCGG, and NNGG). See, for example, Fig. S4 (ESI†) with the distributions for VVGG. The lower deviations of the number of water molecules around the constrained versions relative to the flexible ones for some peptides suggest that restricted chain dynamics may result in changes in hydration water dynamics (Fig. S3, ESI†).

Dynamic properties of hydration water

As explained in the Introduction, THz spectroscopy can probe low-frequency collective motions involving many water molecules at distances of up to 20 Å and more from the protein surface.[53] MD simulations usually indicate a significant retardation of water dynamics only within the first several angstroms (up to 7–8 Å).[53–57] However, such analyses are based on single water molecule dynamics and, of course, cannot be directly compared with the results of THz spectroscopy. Given the minimal conformational effects (our peptides are linear and fixed in space) and relatively small relaxation times of water close to the exposed loop regions in the real proteins,[14] we expected that our analyses of the dynamic characteristics of hydration water will detect the difference in water dynamics only within a few angstroms from the surface of flexible and constrained peptides. However, our analysis showed that restriction of peptide dynamics can affect the dynamics of water at much longer distances (Tables 1 and 2).

We used the survival probability autocorrelation function for the analysis of the water translational dynamics in the hydration shell of the peptides. For all constructed peptides, we analyzed the residence time of water molecules within the first 3.5 Å and 5 Å from the peptide surface. The curves were fitted with a triple exponential function (see Fig. 2 for the RRGG peptide example) $y(t) = ae^{(-t/\tau_1)} + be^{(-t/\tau_2)} + ce^{(-t/\tau_3)}$. The value of R^2 for the fit of all systems was above 0.99.

The average residence times (τ_1, τ_2, τ_3) and amplitude-weighted average water residence times ($\tau_{avg} = a\tau_1 + b\tau_2 + c\tau_3$) of water molecules were calculated (see Tables 1, 2 and Tables S1, S2, ESI,† peptides with certain residues are ordered according to the hydrophobicity scale of their sidechains[112]). Following the fit, water molecules with short ($\tau_1 \approx 1$ ps), intermediate ($\tau_2 \approx 4$–9 ps) and longer ($\tau_3 \approx 10$–30 ps) residence times can be distinguished within 3.5 Å of the peptide surface (*i.e.*, within the first hydration shell). We did not observe a significant fraction of 'slow' water molecules with a residence time ≥ 100 ps even around the restricted peptides. Nevertheless, the difference in residence times for flexible and constrained peptides indicates the presence of stronger interactions between the peptides and their hydration water when peptide dynamics is restricted. The effect was observed within a distance of 3.5 Å and 5 Å for all the peptides. A longer residence time of up to 3 ns was observed upon restraining the peptide dynamics, but the magnitude of the effect varies between different peptides. Although residence times τ_1, τ_2, and τ_3 were longer in the case of the constrained versions of the peptides, the difference in their amplitudes (*a*, *b*, and *c*) meant that for some peptides (QQGG, for example) there was no significant difference in the average residence time of water, τ_{avg}, within 3.5 Å.

Table 1 Amplitude-weighted average residence times (τ_{avg}) of water molecules within a certain distance from the flexible/constrained peptides' surface

Residue[a]	3.5 Å[b] (ps)	Δ[d] (ps)	Δ[e] (%)	5 Å[b] (ps)	Δ[d] (ps)	Δ[e] (%)
I	7.6/9.2	1.6	21	18.3/20.0	1.7	9
V	7.3/7.6	0.3	4	18.0/19.2	1.2	7
L	7.2/8.2	1.0	14	17.9/19.7	1.8	10
F	7.2/8.1	0.9	12	18.5/20.7	2.2	12
C	6.0/6.5	0.5	7	17.3/18.3	1.0	6
M	6.3/6.3	0	0	17.7/19.3	1.6	9
A	6.4/6.7	0.3	6	16.4/17.7	1.3	7
T	7.3/8.4	1.1	14	18.1/20.2	2.1	11
S	6.7/7.4	0.7	10	17.5/18.8	1.3	8
W	7.4/8.2	0.8	12	19.9/22.2	2.3	12
Y	7.5/8.0	0.5	7	19.4/21.2	1.8	9
H	7.0/7.8	0.8	12	18.6/19.9	1.3	7
N	7.3/8.0	0.7	10	19.0/20.5	1.5	8
Q	6.9/6.9	0	0	19.1/20. 7	1.6	8
D	16.2/19.3	3.1	20	24.3/26.8	2.5	11
E	14.0/15.6	1.6	11	23.9/25.6	1.7	7
K	6.7/7.6	0.9	15	19.3/21.0	1.7	9
R	6.8/7.8	1.0	16	20.5/22.6	2.1	10
Bulk[c]	4.8	—	—	7.2	—	—

[a] Residue X in $(XXGG)_5$ peptides. [b] $\tau_{avg} = a\tau_1 + b\tau_2 + c\tau_3$. [c] Residue time of water in the bulk. [d] $\Delta = (\tau_{avg}^{constrained} - \tau_{avg}^{flexible})$. [e] Normalized Δ; $\Delta\tau_{avg}^{normalized} = ((\tau_{avg}^{constrained} - \tau_{avg}^{flexible})/\tau_{avg}^{flexible}) \times 100\%$.

Table 2 Amplitude-weighted average residence times (τ_{avg}, ps) of water molecules within a certain distance from the flexible/constrained peptides' surface

Residue	8 Å	12 Å
T	40.8/44.3	79.8/83.9
W	45.0/49.5	85.6/93.6
E	49.2/51.9	90.2/94.6
R	47.3/50.6	91.5/97.8

Our calculations show that τ_{avg} is 4.8 ps and 7.2 ps within 3.5 Å and 5 Å of the bulk water molecules, respectively, which is significantly lower than for water close to the peptides. In our simulations, we used the SPC/E water model. In order to estimate the effect of the water model used, we performed additional simulations of the RRGG peptide (flexible and constrained forms) using the TIP5P water model. For TIP5P-modeled water molecules, τ_{avg} in bulk was found to be 7.5 ps for a 3.5 Å cutoff and 12.60 ps for a 5 Å cutoff, which is less than the τ_{avg} values of TIP5P-modeled water molecules close to RRGG (see, for example, Tables S3 and S4 for 3.5 Å cutoff, ESI†). Our results showed increased solvation of the RRGG peptide upon using the TIP5P water model compared with the SPC/E water model, with $\tau_{avg}^{TP5P} > \tau_{avg}^{SPC/E}$. For example, for unconstrained RRGG, 11.9 ps for the TIP5P model *vs.* 6.8 ps for the SPC/E model for a 3.5 Å cutoff and 20.8 for the TIP5P model *vs.* 20.5 ps for the SPC/E model for a 5 Å cutoff. However, both water models produce results that are qualitatively similar.

In general, analyzing the survival probability (residence time) of water molecules close to the studied peptides revealed a pronounced increase in retardation of water molecule movement close to the constrained peptides relative to their flexible versions. It is important to emphasize that we calculated the survival probability of water molecules within the hydration shell, which means that if the dynamics of a water molecule is coupled with the dynamics of a peptide, it will stay within the hydration shell when the peptide fluctuates relative to its initial conformation. In other words, the possible effect of coupling between water and solute motions is taken into account in our calculations.

Also, as mentioned in the Methods section, we checked the possible effect of restricted flexibility by choosing a particular

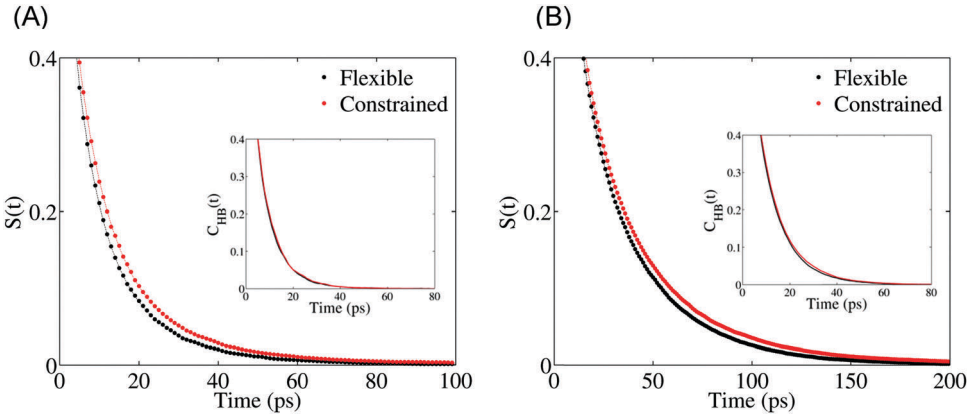

Fig. 2 Autocorrelation functions of water molecules within 3.5 Å (A) and 5 Å (B) of flexible (black) and constrained (red) RRGG peptide versions. Main panels: Survival probability (residence time) of water molecules; insets: H-bond lifetimes. Dots represent simulation data and dashed lines represent a triexponential fit. In the inset, solid lines represent simulation data.

peptide conformation. For each peptide, we chose the conformation whose internal energy was most populated, thus, other conformations with similar internal energy values may affect the hydration water differently. In order to study the effect of the selected conformation, we used two different constrained conformations of the WWGG peptide. The analysis of water residence time within a 3.5 Å cutoff and 5 Å cutoff (as well as other analyses, data not shown) did not reveal a significant difference between the chosen conformations (see, for example, Tables S3 and S4 for 3.5 Å cutoff, ESI†).

Our analysis showed a significant difference in the observed effect for the peptides constructed with different amino acid residues. Significantly longer residence times for water molecules within 3.5 Å and 5 Å cutoffs were observed for the peptides constructed from negatively charged residues D and E (Table 1). D and E residues contain a H-bond-acceptor carboxyl group (COO^-), which can induce a pronounced slowing of hydration water dynamics.[113] For peptides with residues containing H-bond donor groups, as well as for hydrophobic residues, the water retardation effect was less pronounced.

The difference in the water retardation effect arising from the flexible *versus* the constrained version of the peptides also varied for different peptide types (Table 1). For both cutoff distances (3.5 Å and 5 Å), the most pronounced effect was observed upon constraining the peptides with negatively charged residues (D and E). Within a 3.5 Å cutoff distance, a surprisingly strong effect was also observed upon restricting the dynamics of IIGG. Within a 5 Å cutoff distance, the difference in the retardation effect for different peptide types became less significant (see Δ values in Table 1).

To identify the maximum distance from the protein within which restricting the conformational flexibility can affect the translational dynamics of water, we calculated the survival probability of water molecules within longer cutoff distances. We used two additional cutoff distances (8 and 12 Å) for the peptides based on a hydrophobic residue (WWGG), a polar residue (TTGG), and two charged residues: a hydrogen bond donor (RRGG) and an acceptor (EEGG). The results indicated that even at 12 Å away from the peptide surface, the translational dynamics of water was affected by constraining the peptide flexibility (Table 2). Although we did not calculate the corresponding time constants of bulk water for these distances (due to limitations on the box size, see Methods section for details), the difference in values for flexible and constrained peptide versions indirectly indicates that peptides can affect water translational dynamics up to at least 12 Å.

Increasing the cutoff distance for the survival probability calculations increases the residence time of water molecules and the value of $(\tau_{avg}^{constrained} - \tau_{avg}^{flexible})$ can be expected to have a different 'weight' at 3.5, 5.0, 8, and 12 Å cutoffs. Accordingly, in order to estimate the effect of peptide confinement on hydration water at different distances, we calculated normalized values for the amplitude-weighted average water residence time within different cutoff distances,

$$\Delta\tau_{avg}^{normalized} = ((\tau_{avg}^{constrained} - \tau_{avg}^{flexible})/\tau_{avg}^{flexible}) \times 100\%$$

The values calculated for TTGG, WWGG, EEGG, and RRGG showed that the difference in the water retardation effect decreased with distance. This is a general tendency; however some fluctuations are possible (Table 3). It is important to note that these normalized values clearly indicate that retardation of water molecules within the long cutoff distances (>3.5 Å) is not only due of water molecules from the first hydration shell. Otherwise, due to the very fast growth of the number of analyzed water molecules, these values will decrease drastically as a function of distance. Oppositely, we observed quite a smooth decrease of values as a function of time (see Table 3, for not normalized $\Delta\tau_{avg}$ values, see Table S5, ESI†).

Table 3 Normalized values of amplitude-weighted average water residence time (%) within different cutoff distances: $((\tau_{avg}^{constrained} - \tau_{avg}^{flexible})/\tau_{avg}^{flexible}) \times 100\%$

Residue	3.5 Å	5 Å	8 Å	12 Å
T	14.0	7.3	8.5	5.2
W	11.8	7.6	10.0	9.4
E	11.5	10.6	5.5	4.9
R	15.9	9.0	7.0	6.9

Table 4 Amplitude-weighted average H-bond lifetimes (τ_{avg}, ps) of water molecules within 3.5 Å from the flexible/constrained peptides' surface

Residue	3.5 Å	Δ
T	5.4/5.6	0.2
W	6.0/6.4	0.4
E	6.0/6.2	0.2
R	6.0/6.2	0.2
Bulk	4.3	—

In addition, we performed the analysis of residence time of water molecules within the cutoff distances from 8 to 12 Å for the same four peptides. This analysis also showed the difference in τ_{avg} for flexible and constrained variants of peptides (Table S6, ESI†).

Adopting an alternative approach, we analyzed how long it takes for a water molecule to reach a certain distance from the peptide. This analysis showed the same tendency of water molecules to be 'slower' in the vicinity of constrained compared with flexible peptide versions. The effect extended for at least 13 Å from both charged and hydrophobic residues (Fig. S3, ESI†).

Using an autocorrelation function of the water dipole moment vector, we also analyzed the reorientational dynamics of water molecules. The analysis did not reveal any significant difference in the reorientational dynamics of hydration water upon restriction of peptide dynamics (data not shown). We also studied how the restriction of peptide dynamics affected the lifetimes of water–water hydrogen bonds close to the peptide surface. Analysis did not reveal a strong difference between the values of τ_{avg} (calculated similar to survival probability) for water–water H-bonds within 3.5 Å compared with 5 Å from the surface of flexible and constrained versions of the peptides. See Table 4 for τ_{avg} (3.5 Å cutoff) for TTGG, WWGG, EEGG, and RRGG and Fig. 2 (insets). However, the τ_{avg} values of water H-bonds close to the peptides were longer than for the bulk water molecules.

Overall, we find that restricting peptide conformational flexibility affects the translational dynamics of hydration water molecules. The effect can extend until at least 12–13 Å, depending on the chemical nature (amino acid residues) of the peptide. The reorientational dynamics of hydration water and the lifetime of water–water H-bonds are less affected by the restriction of peptide conformational flexibility.

'Slow' water in the hydration shell

As discussed above, many studies indicate the existence of a long relaxation time (in the order of 100 ps or more) for hydration water molecules located close to the protein surface.[12,14,27–30,33–36,44–46] These water molecules can constitute only a few percent of the total number of hydration water molecules. Nevertheless, they may play an important role in stabilizing the protein conformation.[46]

Our analysis of water molecule residence times did not reveal a significant fraction of 'slow' water (SW) molecules. We calculated the number of SW molecules in the first hydration shell of the constructed peptides and found that they constituted only 0.3–0.8% (5–25 molecules) of water molecules within this shell, which is even less than for natural proteins.[46] Such a low population in this cluster may indicate the importance of the spatial conformation of a protein. The linear conformation of the constructed peptides may not efficiently trap water molecules for long periods. As discussed in the Introduction, the observed hydration sites with particularly long residence times ($\geq$80 ps) are located in buried areas of the protein, in cavities and clefts,[14,62] which are absent from our constructed peptides.

Nevertheless, our study showed that, even in the case of the short constructed peptides, the chemical nature and dynamic properties of the chain could affect the residence time and number of SW molecules (Fig. 3). According to the calculations, restricting the flexibility of the chain resulted in an average gain of 2–6 SW molecules. The residence time of SW molecules also slightly increased (by 3–10 ps).

The chemical nature of the peptides defined the magnitude of the effect. Although peptides with some charged residues (D and E) were associated with more of the SW molecules with the longest residence times, we did not observe a correlation between the number of SW molecules (or their residence times) and the hydrophobicity of the residues. In Fig. 3, peptides with certain residues are ordered according to the hydrophobicity scale of their sidechains.[112] The observed difference may be related to the molecular mechanism of H-bond formation between water molecules and the donor/acceptor molecular groups of the solute.[113]

An analysis of the distribution of SW on the surface of the peptides showed that these water molecules could be located

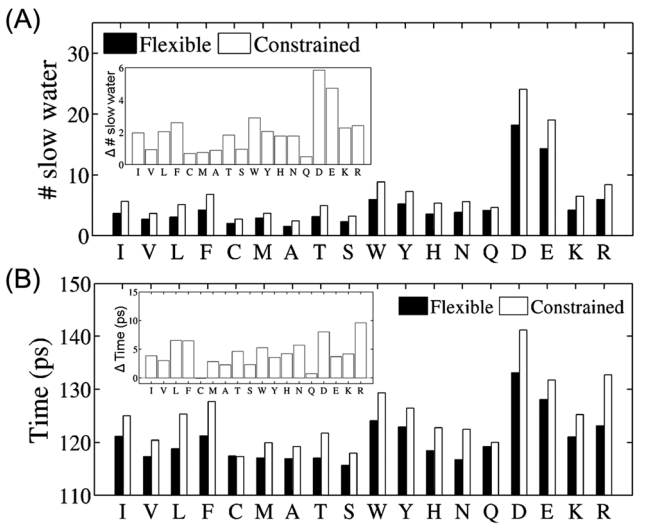

Fig. 3 Analysis of 'slow' water (SW) molecules (residence time $\geq$ 100 ps) close to flexible (black) and constrained (white) peptides. (A) Average number of SW molecules within 3.5 Å of the peptides and (B) average residence time of SW within 3.5 Å of the peptides. Peptides are ordered on the *x*-axis according to the hydrophobicity of the side chains of their residues (see text). The X residue of each XXGG is identified on the *x*-axis label. Insets: The difference between the values for the constrained and flexible peptide versions. The difference between the distributions of residence times and the number of "slow water" molecules in each frame for flexible and constrained versions of the peptides was proven with the *T*-test. For all studied systems, p = 0.001.

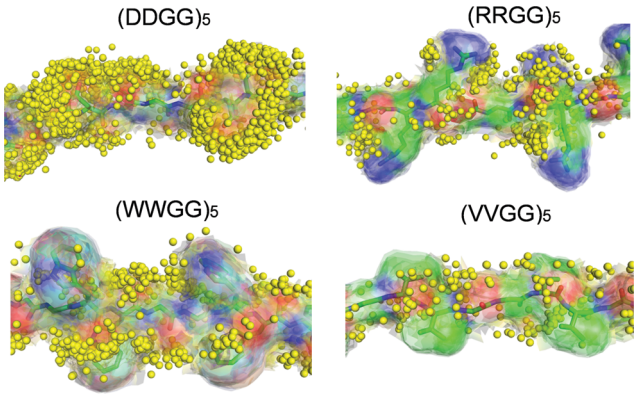

Fig. 4 Visual representation of SW at different sites on the surface of different peptides (constrained versions of DDGG, RRGG, WWGG, and VVGG): alignment of ~200 different conformations. The first conformation is shown as sticks and clouds, the rest as clouds. Water molecules are represented as yellow spheres. For peptides: O, red, N, blue, and C, green.

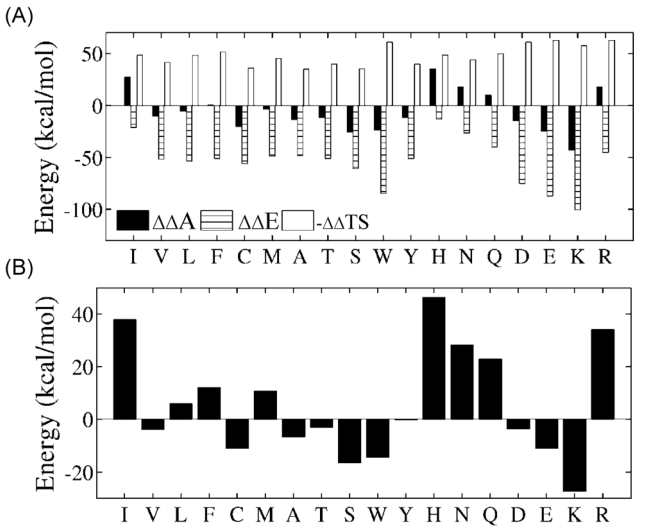

Fig. 5 Thermodynamic parameters of water molecules within 4.5 Å of the peptide surface. All values are shown as ΔΔ (constrained minus flexible): (A) $\Delta\Delta A$, the difference in the Helmholtz hydration free energy (black); $\Delta\Delta E$, the difference in the hydration potential energy (dashed); and $-\Delta\Delta TS$, the difference in the hydration entropic contribution to free energy (white). The identity of X in XXGG appears as the *x*-axis label. (B) The sum of $\Delta\Delta A$ and the difference in the conformational entropy of the side chains of the peptides (ΔTS_{conf}).

not only close to the side chains (which would probably result in correlation with their hydrophobicity) but also close to the backbone (which contains polar oxygen and nitrogen atoms). See, for example, the distribution of SW close to the constrained versions of DDGG, RRGG, WWGG, and VVGG (Fig. 4). This may explain why, for example, the number of SW molecules and their residence time were similar for the peptides constructed with hydrophobic I and charged K. The peptide backbone strongly impacted the solvation of nonpolar side chains. In the presence of the short peptide backbone, nonpolar amino acid chains were less hydrophobic than expected based on the solvation data for free side-chain analog molecules.[72,73] Furthermore, a rather high concentration of SW was noticed close to the C terminals of the peptides. Hydrophilic carboxyl groups (H-bond acceptors) are known to have a pronounced effect on the dynamics of water.[113,114]

Our analysis of SW clusters emphasizes that energetic inhomogeneity is an important factor that affects the hydration water of even short linear peptidic biomolecules.

Thermodynamic characteristics of hydration water

Motivated by estimating the effect of the longer residence time of the hydration shell on the protein stability, we used the GIST method[105] to analyze the thermodynamic properties of water within the first hydration shell of the peptides. In order to improve the statistics for the flexible variants of the peptides, the cutoff distance for the water molecules for this analysis was defined as 4.5 Å, which is slightly larger than the size of the first hydration shell (~3.5 Å). Using this approach, we defined the change in the Helmholtz free energy, the potential energy, and the entropic contribution to the Gibbs free energy (ΔA, ΔE, $-T\Delta S$, respectively) for constrained and flexible peptides, and then calculated the change in the change as $\Delta\Delta = \Delta_{constrained} - \Delta_{flexible}$. A summary of the analysis is presented in Fig. 5a. The validity of the data was checked by splitting the sampled trajectories into several parts and calculating the standard deviations for the thermodynamic values obtained based on this repetitive analysis. According to this approach, the standard deviation of the data for the systems did not exceed 1–2 kcal mol^{-1}. For all the peptides, restricting the chain flexibility significantly affected the thermodynamics of the hydration shell and decreased the hydration water entropy (positive values of $-T\Delta\Delta S$) and potential energy (negative values of $\Delta\Delta E$), which may provide additional evidence for the coupling between protein and water motions. The balance between these contributions in the case of each peptide type defined the resulting contribution of hydration water to the free energy of the system. Similarly to the findings for the residence time and number of SW molecules, the free energy contribution of hydration water did not correlate with the hydrophobicity of the residues. An unfavorable contribution was observed for peptides containing I, H, N, Q, and R, whereas for other peptides the free energy contribution was favorable or almost neutral.

An analysis of the distribution of sites with favorable free energy values (≤ -0.2 kcal mol^{-1}) for hydration water can help elucidate the effect of the chemical nature of the peptides on hydration thermodynamics. As shown in Fig. S6 (ESI†), thermodynamically favorable sites were located close to the polar atoms of the backbone and side chains of different peptide types. Charged residues, especially acceptor oxygens of D (and E), also provided additional strong binding sites for water close to the charged atoms. The distributions of the favorable free energy values were in good agreement with the distribution of the SW on the surface of the peptides (Fig. 4).

In the next step, we sought to estimate how the defined thermodynamic effect of hydration water retardation following the restriction of peptide flexibility could contribute to the stability of real proteins. To quantify the effect of having a flexible loop in comparison to a more rigid structural element,

the configurational entropy of this region (TS_{conf}) should be estimated in addition to their different solvation entropy. The configurational entropic term was added to the hydration free energy of the peptides. Adding this term resulted in a less favorable (or more unfavorable) change in free energy for all the constructed peptides, but it reversed the sign of $\Delta\Delta A$ only in the case of the L, F, and M residues (Fig. 5b).

The different solvation free energy of studied peptides may serve as a prediction for the effect of mutation on stability depending on the local dynamics of the mutated site. To estimate how the substitution of a certain residue could affect the stability of the system, we analyzed a database of $\sim$1000 *in vitro* mutations reported in the literature to enable a broad comparison with our simulated peptides.[115] Since we are interested in the solvation effect, only residues that are solvent exposed were selected resulting in 519 mutants. We expected that the free energy effect of substituting certain residues with A or G in the exposed protein regions may correlate with the difference in hydration free energy observed in our simulations depending whether the residues are located at rigid or flexible regions. For the purpose of comparison, we related the flexible variants of the constructed peptides to the unstructured exposed regions of the proteins and loops while relating the constrained variants to the structured exposed regions of the proteins. This relation is very notional and was performed solely to obtain a very general estimation.

In Fig. 6, we show the distribution of the values for the change in the free energy of protein stability following the mutation of certain residues to A or G in the exposed loops or α-helices of the proteins. The data were divided into two groups of mutations: (a) K, E, D, C and W, and (b) V, L, I, F, H and M. We found that the mutation of K, E, D, C and W to A/G usually resulted in protein destabilization. Destabilization was stronger in the structured α-helices. Mutation of V, L, I, F, H and M to A/G also usually resulted in destabilization of the protein, however in this case destabilization was stronger when the mutated residues are in the loop region of the proteins than in the α-helical regions.

Our analysis showed that, for peptides comprising residues from the first group (K, E, D, C and W), hydration water was characterized by a favorable free energy upon restriction (compared with the structured alpha helices); for the peptides comprising residues from the second group (V, L, I, F, H and M), hydration water was characterized mostly by unfavorable free energy upon restriction (compared with the loops).

The qualitative agreement observed between the computed hydration free energy difference for some of the peptides ($\Delta\Delta A$) and the *in vitro* observed difference of free energy upon mutations in α-helices and loop regions (the difference in the distributions of $\Delta\Delta G$ values, in the case of loops and helices) emphasizes the important contribution of hydration water to the free energy of the system. This contribution is related to the changes in the dynamics of hydration water molecules close to the biomolecule surface, which is characterized by chemical and conformational inhomogeneity. Accordingly, this initial attempt to correlate between protein flexibility, thermodynamic stability and solvation properties suggests that the effect of mutation is sensitive to the local dynamics of the protein backbone which affects the solvation free energy of that site.

Discussion

The effect of short peptides and amino acids on hydration water has been studied previously. Such a system is a useful model for understanding how the basic chemical, structural, and dynamic properties of biomolecules can affect (or be affected by) hydration water. Previous studies of short peptides and amino acids showed that both the chemical nature and the conformational properties of the peptides and constituting residues can significantly affect their hydration properties.[18,54,71–73,113,116–119]

In the current study, we focused on the effect of chain flexibility on hydration properties. We constructed 18 amino acid residue peptides with the sequence XXGG repeated five times, where X represents one of the common amino acids other than glycine or proline. Through MD simulations of the

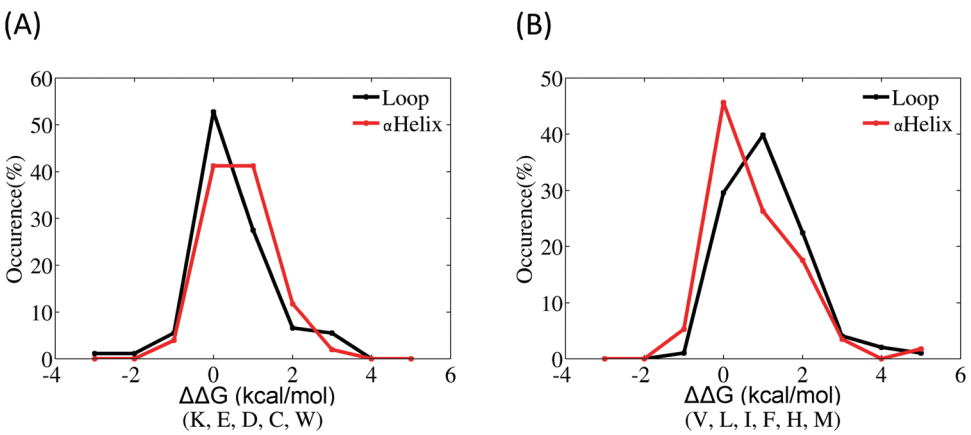

Fig. 6 Effect of a mutation located in the exposed loops or α-helices of the proteins. (A) Distribution of the values for the change in the free energy of protein stability ($\Delta\Delta G$) for substituting K, E, D, C, or W for A or G; (B) distribution of $\Delta\Delta G$ values for substituting V, L, I, F, H, or M for A/G. Black, loop and unstructured regions; red, α helices.

short peptides, we showed how restricting peptide chain flexibility can affect the structural, dynamic, and thermodynamic properties of hydration water. Our analyses showed that the structural properties of water are affected by the presence of the peptide chain, although restricting chain flexibility did not result in a significant difference in the time-averaged structural properties of hydration water molecules. Analyses of the dynamic properties of water revealed a significant difference between water molecules close to the constrained variants of the peptides compared with those close to the flexible peptide variants. The previously mentioned experimental, computational, and theoretical studies[12–20,22,23] suggested the presence of coupling between the motions of water and proteins.

In order to improve our understanding of hydration water dynamics close to the constructed peptides, we considered the specific effects of water models. In our simulations we used the SPC/E water model. Specific analysis of water models revealed that the SPC/E water model gives the best bulk water dynamics and structure.[102] For the SPC/E model, τ_{avg} = 3.2–6 ps (depending on the residence time calculation method applied).[120] Our calculations showed that τ_{avg} within 3.5 Å for the bulk water molecules is 4.84 ps, which is within the range found by others using this model. A study of the dynamic and solvation properties of small oligopeptides revealed significant differences in the specific solvation for different water models.[121] The authors concluded that the choice of the water model may affect the dynamics of the flexible parts of the proteins that are solvent-exposed. We found that the difference in solvation for the flexible compared with the constrained RRGG peptide was qualitatively similar for the SPC/E and TIP5P water models, however solvation of the RRGG peptide using the TIP5P water model was higher compared with that using the SPC/E water model ($\tau_{avg}^{TP5P} > \tau_{avg}^{SPC/E}$).

The analysis of the residence time (survival probability) of water molecules within different cutoff distances (3.5, 5, 8, and 12 Å) from the peptide surface revealed that the restriction of peptide chain flexibility can slow down water translational motions to a distance of at least 12–13 Å. In another computational study, measurements of tagged molecule potential energy (TPE), which corresponds to the interaction energy of individual water molecules with all the other molecules in the system, showed a 2–5% difference in the energy of the bulk water compared with water close to the short peptides.[118] Strong TPE correlated with longer residence times for water molecules and depended on the chemical nature of the closest amino acid residue. The oscillatory values of the computed TPE for water in the presence of the peptide extended to at least 10 Å. It was asked whether the long-range effect of the energetics of water molecules located close to the peptide is somehow related to the existence of the very large ($\sim$20 Å) dynamic hydration shell around biomolecules observed by THz spectroscopy.[118] Consistent with this notion, the computational and experimental studies of folded peptides, proteins, and hydrophilic surfaces also revealed a spatial correlation between protein and water dielectric properties at distances much greater than 10 Å.[18,59,60,122,123] In this sense, our results suggest that the conformational flexibility of biological molecules (measured here for linear peptides) should be considered sufficient to affect the properties of hydration water.

A stronger retardation of water dynamics and increased numbers of affected water molecules were shown in the vicinity of hydrophilic compared with hydrophobic amino acids and short peptides using THz spectroscopy and MD simulations.[54,119] Our results are in agreement with these observations, suggesting a different range of retardation effects around peptides with different chemical natures. A possible mechanism for such differences, at least within the first hydration shell, was suggested by the extended jump model. According to the model, H-bond acceptor groups induce an additional transition state (which is missing in the case of H-bond donors and hydrophobic groups) that can dramatically change the water dynamics by increasing the free energy barrier between protein–water and water–water H-bonds. Strong H-bond acceptors (COO^-) induce a pronounced slowdown of hydration water dynamics.[66–69,113] However, it was suggested that a stronger influence of proteins, peptides and single lysine residues on water (compared to small hydrophobic molecules and sugars) may be attributed to a nontrivial mixture of effects related to the presence of polar groups, residues with amphiphilic character, and frustration, rather than to the simple addition of the effects of the hydrophobic and hydrophilic parts of a molecule.[71] Thus, the study of the peptide backbone effect on the solvation thermodynamics of amino acid side chains showed that all nonpolar side chains attached to a short peptide backbone are considerably less hydrophobic than the free side chain analog molecules. By contrast, the hydrophilicity of the polar side chains is hardly affected by the backbone.[72] Such a difference is related to the changes in the balance between solvation entropy and enthalpy.[73] The effect of protein dynamics restriction considered in our study also showed a dependence on the chemical nature of the peptides, being stronger for the negatively charged residues (D and E) within 3.5 Å. However, in general, the effect that constraining the peptide had on hydration water did not significantly correlate with residue hydrophobicity. For example, the effect of conformational restriction as a function of distance was within the same range for the peptides having a different chemical nature (Table 3). It is possible to speculate that a backbone with nonpolar side chains may exert a compensational effect that decreases the difference in the water retardation effect arising from peptides with a different chemical nature.

Our analyses of the reorientational dynamics of hydration water and the lifetime of hydrogen bonds did not reveal an effect of peptide restriction. This finding is in agreement with previously reported results which showed that the rotational dynamics of water on the protein surface is shaped mostly by electrostatic interactions, without a strong effect of protein flexibility.[65] However, our results did not show a significant retardation of water reorientational dynamics close to the peptides with the charged residues either. Thus, we did not observe a marked difference in the reorientational dynamics of water close to charged compared with nonpolar residues, for example. This may be related to the additional effect of the

polar atoms of the main chain and to the very simple (linear) conformations of the short constructed peptides.

Water molecules with a long relaxation time (100 ps or more) can constitute only a few percent of the total number of hydration water molecules,[12,14,27–30,33–36,44–46] however they may significantly stabilize the protein conformation.[46] Furthermore, the analysis of SW distribution helps to define the most favorable hydration sites. We therefore specifically analyzed the cluster of SW molecules close to the constructed peptides. Our analysis did not reveal the presence of a significant amount of SW close to the peptides, even in the case of peptides constructed with charged residues (for which the value was $<1\%$). This may indicate the importance of the local environment (*e.g.*, secondary and tertiary structures) in hydration water dynamics. However, the number of such water molecules and their residence time is different for different residue types and can be increased by fully constraining the peptide backbone. Analysis of the distribution of SW on the peptide surface provides a visual indication of the importance of the chemical nature of the studied peptides. In addition to an obvious tendency of SW to concentrate close to charged groups, we observed a significant fraction of SW close to the main chain of the peptides. As discussed in the Results section, this may explain the observed small difference in SW characteristics between peptides constructed with hydrophobic and some charged residues (I and K, for example). These results are in good agreement with the role played by the main chain and the general chemical environment in hydration water effects (see above). Analysis of the SW cluster underlines the important role of the chemical nature of all the groups present (including the main chain) in the hydration effects of a biomolecule, even at the level of small linear peptides.

The release of hydration water into the bulk can yield a significant contribution to the free energy.[46,124] Our simple thermodynamic analysis showed that restricting peptide dynamics may affect the thermodynamic parameters of hydration water. Such a restriction decreases the hydration water entropy and energy, which may serve as an indication of protein–water coupling. The balance between these contributions for different residue types defines the favorable or unfavorable contribution to the free energy of the system upon restricting the conformational dynamics of the peptide chain. This analysis of a mutation database revealed that mutations in exposed sites can result in different thermodynamic effects for different residues and that this effect is different in the loop and helical regions due to different responses of the solvent to the backbone flexibility. We found some correlation between the changes in hydration free energy upon restriction of peptides constructed with different residues and the effect of *in vitro* mutations of different residues in exposed protein regions that are more or less structured.

Conclusion

In the current study, we investigated the effect of chain flexibility on the hydration properties of various peptides. We designed 18 peptides with the repeat sequence XXGG, where X represents one of the common amino acids other than glycine and proline. To avoid structural heterogeneity, we kept the protein backbone extended. Furthermore, the sequence was selected to avoid interactions between neighboring side chains. Accordingly, the peptides were designed to maximize the exposure of the side chains to the solvent. The simplicity of the structure and the sequences of these peptides should allow the crosstalk between hydration dynamics and protein flexibility to be dissected. Using MD simulations, we studied how restricting peptide flexibility can affect the structural, dynamic, and thermodynamic properties of the hydration water. In contrast to time-averaged structural properties, analyses of the dynamic properties of water showed a significant difference for water molecules close to the constrained peptides compared with the flexible variants. Restriction of peptide chain flexibility can slow down water translational motions to a distance of at least 12–13 Å, while the effect on reorientational dynamics and hydrogen bond lifetime was insignificant. Analysis of the 'slow' water cluster revealed the importance of the chemical nature of all the groups present (including the main chain) in the hydration effects, even for small linear peptides. Our thermodynamic analysis of hydration water revealed that an unfavorable decrease in solvent entropy around rigid peptides is balanced by a decrease in enthalpy. This balance is not perfect and depends on the peptide sequence. It can result in either a positive or negative free energy change due to protein–solvent interactions. We also tried to estimate how the defined thermodynamic effect can contribute to the stability of real proteins. We found some correlation between the changes in hydration free energy upon restriction of protein dynamics and the effect of mutations in the more and less structured exposed regions of the proteins.

Our constructed peptides can, to some extent, be compared to IDPs. It was shown that the faster motions of hydration water around IDPs compared with ordered globular proteins can largely be attributed to the greater flexibility of the former, rather than their relatively weaker interactions with the solvent.[92] The high conformational flexibility of IDPs facilitates greater mobility of the surrounding water molecules, while confining them within the hydration layer.[56] It seems that more than their increased flexibility, it is the exposure and abundance of charged residues in IDPs that affect their hydration properties. Charged residues cause IDPs to bind more water molecules than globular proteins, and these water molecules are more ordered and characterized by a longer residence time within the hydration layer in IDPs.[56] Moreover, previously it was shown that increased protein motion reduces the retardation of water dynamics that is caused by an increase in the translational space and acceleration of water following orientational decoupling.[65] Water molecules located close to the protein surface can jump to the sites previously occupied by other water molecules or by protein groups. The second possibility is blocked in the case of constrained proteins.[65] In agreement with these previous results for proteins,[65] the residence time of water molecules, measured in our study, was longer for the constrained variants of the peptides. Yet, we show that the thermodynamic consequence of the higher mobility of water around the flexible peptides

depends on the identity of the amino acids suggesting a complex effect on the free energy of IDPs.

For peptides with negatively charged residues, the retardation of water dynamics was more pronounced; however, the difference in the hydration water dynamics upon constraining short peptides of a different chemical nature did not correlate with the hydrophobicity of the peptide sidechains. Additional factors, such as the presence of polar groups in the main chain of the peptides and, possibly, the bulkiness of the side chains may play a significant role in solvation effects. Our study suggests that different regions of the proteins that have different configurational entropies (*e.g.*, loops *vs.* α-helices or β-sheets) may also have different solvation entropies and therefore different solvation free energy contributions to the overall thermodynamic stability. Also, mutating the same type of residue may have different effects on stability depending on the flexibility of the site. It is suggested that this effect should be considered, for example, in protein design approaches.

Acknowledgements

This work was supported by the Kimmelman Center for Macromolecular Assemblies and the Minerva Foundation, with funding from the Federal German Ministry for Education and Research. Support for this research was also provided by the Benoziyo Fund for the Advancement of Science. Y. L. is the Morton and Gladys Pickman Professional Chair in Structural Biology.

References

1 M. Chaplin, *Nat. Rev. Mol. Cell Biol.*, 2006, **7**, 861–866.
2 P. Ball, *Chem. Rev.*, 2008, **108**, 74–108.
3 T. Vajda and A. Perczel, *J. Pept. Sci.*, 2014, **20**, 747–759.
4 M. C. Bellissent-Funel, A. Hassanali, M. Havenith, R. Henchman, P. Pohl, F. Sterpone, D. van der Spoel, Y. Xu and A. E. Garcia, *Chem. Rev.*, 2016, **116**, 7673–7697.
5 D. P. Zhong, S. K. Pal and A. H. Zewail, *Chem. Phys. Lett.*, 2011, **503**, 1–11.
6 Y. Levy and J. N. Onuchic, *Annu. Rev. Biophys. Biomol. Struct.*, 2006, **35**, 389–415.
7 J. Dielmann-Gessner, M. Grossman, V. C. Nibali, B. Born, I. Solomonov, G. B. Fields, M. Havenith and I. Sagi, *Proc. Natl. Acad. Sci. U. S. A.*, 2014, **111**, 17857–17862.
8 M. Grossman, B. Born, M. Heyden, D. Tworowski, G. B. Fields, I. Sagi and M. Havenith, *Nat. Struct. Mol. Biol.*, 2011, **18**, U1102–U1113.
9 Y. Levy and J. N. Onuchic, *Proc. Natl. Acad. Sci. U. S. A.*, 2004, **101**, 3325–3326.
10 G. A. Papoian, J. Ulander, M. P. Eastwood, Z. Luthey-Schulten and P. G. Wolynes, *Proc. Natl. Acad. Sci. U. S. A.*, 2004, **101**, 3352–3357.
11 G. A. Papoian, J. Ulander and P. G. Wolynes, *J. Am. Chem. Soc.*, 2003, **125**, 9170–9178.
12 G. Schiro, Y. Fichou, F. X. Gallat, K. Wood, F. Gabel, M. Moulin, M. Hartlein, M. Heyden, J. P. Colletier, A. Orecchini, A. Paciaroni, J. Wuttke, D. J. Tobias and M. Weik, *Nat. Commun.*, 2015, **6**, 6490.
13 V. Helms, *ChemPhysChem*, 2007, **8**, 23–33.
14 L. Y. Zhang, Y. Yang, Y. T. Kao, L. J. Wang and D. P. Zhong, *J. Am. Chem. Soc.*, 2009, **131**, 10677–10691.
15 H. Frauenfelder, G. Chen, J. Berendzen, P. W. Fenimore, H. Jansson, B. H. McMahon, I. R. Stroe, J. Swenson and R. D. Young, *Proc. Natl. Acad. Sci. U. S. A.*, 2009, **106**, 5129–5134.
16 R. D. Young and P. W. Fenimore, *Biochim. Biophys. Acta, Proteins Proteomics*, 2011, **1814**, 916–921.
17 V. C. Nibali, G. D'Angelo, A. Paciaroni, D. J. Tobias and M. Tarek, *J. Phys. Chem. Lett.*, 2014, **5**, 1181–1186.
18 K. F. Rinne, J. C. F. Schulz and R. R. Netz, *J. Chem. Phys.*, 2015, **142**, 215104.
19 A. L. Tournier, J. C. Xu and J. C. Smith, *Biophys. J.*, 2003, **85**, 1871–1875.
20 M. Tarek and D. J. Tobias, *Phys. Rev. Lett.*, 2002, **88**, 138101.
21 P. W. Fenimore, H. Frauenfelder, B. H. McMahon and F. G. Parak, *Proc. Natl. Acad. Sci. U. S. A.*, 2002, **99**, 16047–16051.
22 F. X. Gallat, A. Laganowsky, K. Wood, F. Gabel, L. van Eijck, J. Wuttke, M. Moulin, M. Hartlein, D. Eisenberg, J. P. Colletier, G. Zaccai and M. Weik, *Biophys. J.*, 2012, **103**, 129–136.
23 S. Khodadadi, J. H. Roh, A. Kisliuk, E. Mamontov, M. Tyagi, S. A. Woodson, R. M. Briber and A. P. Sokolov, *Biophys. J.*, 2010, **98**, 1321–1326.
24 K. L. Ngai, S. Capaccioli and A. Paciaroni, *Biochim. Biophys. Acta, Gen. Subj.*, 2017, **1861**, 3553–3563.
25 K. L. Ngai, S. Capaccioli and A. Paciaroni, *Chem. Phys.*, 2013, **424**, 37–44.
26 S. Capaccioli, K. L. Ngai, S. Ancherbak and A. Paciaroni, *J. Phys. Chem. B*, 2012, **116**, 1745–1757.
27 D. Zhong, *Advances in Chemical Physics*, John Wiley & Sons, Inc., 2009, ch. 3, pp. 83–149, DOI: 10.1002/9780470508602.
28 L. Zhao, S. K. Pal, T. B. Xia and A. H. Zewail, *Angew. Chem., Int. Ed.*, 2004, **43**, 60–63.
29 S. K. Pal, J. Peon and A. H. Zewail, *Proc. Natl. Acad. Sci. U. S. A.*, 2002, **99**, 1763–1768.
30 S. K. Pal and A. H. Zewail, *Chem. Rev.*, 2004, **104**, 2099–2123.
31 R. Abseher, H. Schreiber and O. Steinhauser, *Proteins*, 1996, **25**, 366–378.
32 M. C. Moron, *Phys. Chem. Chem. Phys.*, 2012, **14**, 15393–15399.
33 M. Settles and W. Doster, *Faraday Discuss.*, 1996, **103**, 269–279.
34 W. Doster and M. Settles, *Biochim. Biophys. Acta*, 2005, **1749**, 173–186.
35 D. S. Grebenkov, Y. A. Goddard, G. Diakova, J. P. Korb and R. G. Bryant, *J. Phys. Chem. B*, 2009, **113**, 13347–13356.
36 T. P. Li, A. A. P. Hassanali, Y. T. Kao, D. P. Zhong and S. J. Singer, *J. Am. Chem. Soc.*, 2007, **129**, 3376–3382.
37 S. Ghosh, K. Sahu, S. K. Mondal, P. Sen and K. Bhattacharyya, *J. Chem. Phys.*, 2006, **125**, 204905.
38 K. Bhattacharyya, *Acc. Chem. Res.*, 2003, **36**, 95–101.

39 K. Sahu, S. K. Mondal, S. Ghosh and K. Bhattacharyya, *Bull. Chem. Soc. Jpn.*, 2007, **80**, 1033–1043.
40 K. Bhattacharyya, *Chem. Commun.*, 2008, 2848–2857, DOI: 10.1039/b800278a.
41 M. H. Jia, J. Yang, Y. Z. Qin, D. H. Wang, H. F. Pan, L. J. Wang, J. H. Xu and D. P. Zhong, *J. Phys. Chem. Lett.*, 2015, **6**, 5100–5105.
42 A. A. Golosov and M. Karplus, *J. Phys. Chem. B*, 2007, **111**, 1482–1490.
43 J. N. Scott and P. R. Callis, *J. Phys. Chem. B*, 2013, **117**, 9598–9605.
44 B. Bagchi, *Chem. Phys. Lett.*, 2012, **529**, 1–9.
45 X. J. Jordanides, M. J. Lang, X. Y. Song and G. R. Fleming, *J. Phys. Chem. B*, 1999, **103**, 7995–8005.
46 S. Roy and B. Bagchi, *J. Phys. Chem. B*, 2012, **116**, 2958–2968.
47 J. Qvist, E. Persson, C. Mattea and B. Halle, *Faraday Discuss.*, 2009, **141**, 131–144.
48 J. R. Helliwell, A. Kornyshev, B. Halle and J. B. F. N. Engberts, *Philos. Trans. R. Soc., B*, 2004, **359**, 1223–1224.
49 B. Halle, *Philos. Trans. R. Soc., B*, 2004, **359**, 1207–1223.
50 B. Halle and L. Nilsson, *J. Phys. Chem. B*, 2009, **113**, 8210–8213.
51 S. Ebbinghaus, S. J. Kim, M. Heyden, X. Yu, U. Heugen, M. Gruebele, D. M. Leitner and M. Havenith, *Proc. Natl. Acad. Sci. U. S. A.*, 2007, **104**, 20749–20752.
52 V. C. Nibali and M. Havenith, *J. Am. Chem. Soc.*, 2014, **136**, 12800–12807.
53 M. Heyden and M. Havenith, *Methods*, 2010, **52**, 74–83.
54 G. Niehues, M. Heyden, D. A. Schmidt and M. Havenith, *Faraday Discuss.*, 2011, **150**, 193–207.
55 D. R. Nutt and J. C. Smith, *J. Am. Chem. Soc.*, 2008, **130**, 13066–13073.
56 P. Rani and P. Biswas, *J. Phys. Chem. B*, 2015, **119**, 13262–13270.
57 S. K. Sinha, M. Jana, K. Chakraborty and S. Bandyopadhyay, *J. Chem. Phys.*, 2014, **141**, 22D502.
58 M. Heyden and D. J. Tobias, *Phys. Rev. Lett.*, 2013, **111**, 218101.
59 M. Heyden, D. J. Tobias and D. V. Matyushov, *J. Chem. Phys.*, 2012, **137**, 235103.
60 O. Sushko, R. Dubrovka and R. S. Donnan, *J. Chem. Phys.*, 2015, **142**, 055101.
61 D. Russo, R. K. Murarka, J. R. Copley and T. Head-Gordon, *J. Phys. Chem. B*, 2005, **109**, 12966–12975.
62 V. A. Makarov, B. K. Andrews, P. E. Smith and B. M. Pettitt, *Biophys. J.*, 2000, **79**, 2966–2974.
63 S. Bandyopadhyay, S. Chakraborty, S. Balasubramanian and B. Bagchi, *J. Am. Chem. Soc.*, 2005, **127**, 4071–4075.
64 S. Bandyopadhyay, S. Chakraborty and B. Bagchi, *J. Phys. Chem. B*, 2006, **110**, 20629–20634.
65 F. Pizzitutti, M. Marchi, F. Sterpone and P. J. Rossky, *J. Phys. Chem. B*, 2007, **111**, 7584–7590.
66 A. C. Fogarty and D. Laage, *J. Phys. Chem. B*, 2014, **118**, 7715–7729.
67 D. Laage, G. Stirnemann, F. Sterpone and J. T. Hynes, *Acc. Chem. Res.*, 2012, **45**, 53–62.
68 D. Laage, G. Stirnemann, F. Sterpone, R. Rey and J. T. Hynes, *Annu. Rev. Phys. Chem.*, 2011, **62**, 395–416.
69 F. Sterpone, G. Stirnemann and D. Laage, *J. Am. Chem. Soc.*, 2012, **134**, 4116–4119.
70 L. R. Murphy, N. Matubayasi, V. A. Payne and R. M. Levy, *Folding Des.*, 1998, **3**, 105–118.
71 L. Comez, L. Lupi, A. Morresi, M. Paolantoni, P. Sassi and D. Fioretto, *J. Phys. Chem. Lett.*, 2013, **4**, 1188–1192.
72 T. Hajari and N. F. A. van der Vegt, *J. Phys. Chem. B*, 2014, **118**, 13162–13168.
73 T. Hajari and N. F. A. van der Vegt, *J. Chem. Phys.*, 2015, **142**, 144502.
74 S. K. Sinha and S. Bandyopadhyay, *J. Chem. Phys.*, 2012, **136**, 185102.
75 C. B. Marshall, M. M. Tomczak, S. Y. Gauthier, M. J. Kuiper, C. Lankin, V. K. Walker and P. L. Davies, *Biochemistry*, 2004, **43**, 148–154.
76 E. Duboue-Dijon and D. Laage, *J. Chem. Phys.*, 2014, **141**, 22D529.
77 Y. Xu, R. Gnanasekaran and D. M. Leitner, *J. At., Mol., Opt. Phys.*, 2012, **2012**, 6.
78 A. Kuffel, D. Czapiewski and J. Zielkiewicz, *J. Chem. Phys.*, 2014, **141**, 055103.
79 K. A. Sharp, *J. Chem. Phys.*, 2014, **141**, 22D510.
80 M. J. Kuiper, C. J. Morton, S. E. Abraham and A. Gray-Weale, *eLife*, 2015, **4**, e05142.
81 K. Meister, S. Ebbinghaus, Y. Xu, J. G. Duman, A. DeVries, M. Gruebele, D. M. Leitner and M. Havenith, *Proc. Natl. Acad. Sci. U. S. A.*, 2013, **110**, 1617–1622.
82 S. Ebbinghaus, K. Meister, M. B. Prigozhin, A. L. DeVries, M. Havenith, J. Dzubiella and M. Gruebele, *Biophys. J.*, 2012, **103**, L20–L22.
83 S. Ebbinghaus, K. Meister, B. Born, A. L. DeVries, M. Gruebele and M. Havenith, *J. Am. Chem. Soc.*, 2010, **132**, 12210–12211.
84 U. S. Midya and S. Bandyopadhyay, *J. Phys. Chem. B*, 2014, **118**, 4743–4752.
85 P. Sen, S. Mukherjee, P. Dutta, A. Halder, D. Mandal, R. Banerjee, S. Roy and K. Bhattacharyya, *J. Phys. Chem. B*, 2003, **107**, 14563–14568.
86 S. Pal, K. Chakraborty, P. Khatua and S. Bandyopadhyay, *J. Chem. Phys.*, 2015, **142**, 055102.
87 S. Pal and S. Bandyopadhyay, *J. Chem. Phys.*, 2013, **139**, 235101.
88 B. Born, S. J. Kim, S. Ebbinghaus, M. Gruebele and M. Havenith, *Faraday Discuss.*, 2009, **141**, 161–173.
89 S. Ebbinghaus, S. J. Kim, M. Heyden, X. Yu, M. Gruebele, D. M. Leitner and M. Havenith, *J. Am. Chem. Soc.*, 2008, **130**, 2374–2375.
90 A. H. Mao, S. L. Crick, A. Vitalis, C. L. Chicoine and R. V. Pappu, *Proc. Natl. Acad. Sci. U. S. A.*, 2010, **107**, 8183–8188.
91 A. Marcovitz, A. Naftaly and Y. Levy, *J. Chem. Phys.*, 2015, **142**, 085102.
92 J. C. Jose, P. Khatua, N. Bansal, N. Sengupta and S. Bandyopadhyay, *J. Phys. Chem. B*, 2014, **118**, 11591–11604.
93 S. Pal and S. Bandyopadhyay, *Chem. Phys.*, 2013, **420**, 35–43.

94 S. Pal and S. Bandyopadhyay, *Langmuir*, 2013, **29**, 1162–1173.
95 S. Pal and S. Bandyopadhyay, *J. Phys. Chem. B*, 2013, **117**, 5848–5856.
96 T. P. Li, A. A. Hassanali and S. J. Singer, *J. Phys. Chem. B*, 2008, **112**, 16121–16134.
97 Schrodinger, LLC, unpublished work.
98 K. Lindorff-Larsen, S. Piana, K. Palmo, P. Maragakis, J. L. Klepeis, R. O. Dror and D. E. Shaw, *Proteins*, 2010, **78**, 1950–1958.
99 D. Van Der Spoel, E. Lindahl, B. Hess, G. Groenhof, A. E. Mark and H. J. Berendsen, *J. Comput. Chem.*, 2005, **26**, 1701–1718.
100 B. Hess, H. Bekker, H. J. C. Berendsen and J. G. E. M. Fraaije, *J. Comput. Chem.*, 1997, **18**, 1463–1472.
101 G. Bussi, D. Donadio and M. Parrinello, *J. Chem. Phys.*, 2007, **126**, 014101.
102 P. Mark and L. Nilsson, *J. Phys. Chem. A*, 2001, **105**, 9954–9960.
103 M. Marchi, F. Sterpone and M. Ceccarelli, *J. Am. Chem. Soc.*, 2002, **124**, 6787–6791.
104 P. L. Chau and A. J. Hardwick, *Mol. Phys.*, 1998, **93**, 511–518.
105 T. Luchko, S. Gusarov, D. R. Roe, C. Simmerling, D. A. Case, J. Tuszynski and A. Kovalenko, *J. Chem. Theory Comput.*, 2010, **6**, 607–624.
106 D. W. Li and R. Bruschweiler, *Phys. Rev. Lett.*, 2009, **102**, 118108.
107 D. W. Li, S. A. Showalter and R. Bruschweiler, *J. Phys. Chem. B*, 2010, **114**, 16036–16044.
108 M. C. Baxa, E. J. Haddadian, A. K. Jha, K. F. Freed and T. R. Sosnick, *ACS Chem. Biol.*, 2012, **134**, 15929–15936.
109 M. C. Baxa, E. J. Haddadian, J. M. Jumper, K. F. Freed and T. R. Sosnick, *Proc. Natl. Acad. Sci. U. S. A.*, 2014, **111**, 15396–15401.
110 J. Numata and E. W. Knapp, *J. Chem. Theory Comput.*, 2012, **8**, 1235–1245.
111 K. W. Harpole and K. A. Sharp, *J. Phys. Chem. B*, 2011, **115**, 9461–9472.
112 J. Kyte and R. F. Doolittle, *J. Mol. Biol.*, 1982, **157**, 105–132.
113 F. Sterpone, G. Stirnemann, J. T. Hynes and D. Laage, *J. Phys. Chem. B*, 2010, **114**, 2083–2089.
114 A. Ghosh and R. M. Hochstrasser, *Chem. Phys.*, 2011, **390**, 1–13.
115 R. Guerois, J. E. Nielsen and L. Serrano, *J. Mol. Biol.*, 2002, **320**, 369–387.
116 A. Kuffel and J. Zielkiewicz, *J. Phys. Chem. B*, 2008, **112**, 15503–15512.
117 D. Czapiewski and J. Zielkiewicz, *J. Phys. Chem. B*, 2010, **114**, 4536–4550.
118 M. Agarwal, H. R. Kushwaha and C. Chakravarty, *J. Phys. Chem. B*, 2010, **114**, 651–659.
119 D. Russo, G. Hura and T. Head-Gordon, *Biophys. J.*, 2004, **86**, 1852–1862.
120 D. Laage and J. T. Hynes, *J. Phys. Chem. B*, 2008, **112**, 7697–7701.
121 P. Florova, P. Sklenovsky, P. Banas and M. Otyepka, *J. Chem. Theory Comput.*, 2010, **6**, 3569–3579.
122 G. H. Pollack, *The Fourth Phase of Water: Beyond Solid, Liquid and Vapor*, Ebner and Sons, Seattle, WA, 2013.
123 J. Zheng and G. Pollack, in *Water and the Cell*, ed. G. Pollack, I. Cameron and D. Wheatley, Springer, Netherlands, 2006, ch. 8, pp. 165–174, DOI: 10.1007/1-4020-4927-7_8.
124 C. N. Nguyen, T. K. Young and M. K. Gilson, *J. Chem. Phys.*, 2012, **137**, 044101.